Multipartite entanglement classes of a multiport beam splitter

F. E. S. Steinhoff [*]

Faculdade de Ciência e Tecnologia, Universidade Federal de Mato Grosso, 78060-900 Várzea Grande, Mato Grosso, Brazil

(Received 31 March 2024; accepted 15 July 2024; published 6 August 2024)

The states generated by a multiport beam splitter usually display genuine multipartite entanglement between the many spatial modes. Here we investigate the different classes of multipartite entangled states that arise in this practical situation, working within the paradigm of stochastic local operations with classical communication. We highlight three scenarios, one where the multipartite entanglement classes follow a total number hierarchy, another where the various classes follow a nonclassicality degree hierarchy, and a third one that is a combination of the previous two. Moreover, the multipartite entanglement of higher-dimensional versions of Dicke states relates naturally to our results.

DOI: 10.1103/PhysRevA.110.022409

I. INTRODUCTION

Multipartite entanglement is a fundamental property of quantum systems, enabling the success of tasks that would be unthinkable classically [1–4]. It has deep connections to many-body physics [5,6] as well as foundational aspects of quantum theory [7]. In the paradigm of stochastic local operations with classical communication (SLOCC), there are inequivalent classes of multipartite entangled states, each class having radically distinct physical and informational properties [8]. A considerable number of criteria have been developed to address the problem of SLOCC classification [9–14], which is known to be highly nontrivial from a computational point of view.

In the realm of quantum optics, a multiport beam splitter (MBS) can be employed for the generation of certain specific multipartite entangled states [15,16]. Our approach in the present work, however, is to consider typical output states of a MBS and to then determine the SLOCC classes that arise in this practical scenario. These multimode entangled states are the result of the action of the MBS on a single-mode input state, revealing nonclassical features of this state [17–20].

The paper is divided as follows. In Sec. II, we give a brief review of the problem of SLOCC classification in general, as well as the main features of a multiport beam splitter. In Sec. III, we show various results concerning the multipartite entanglement classes of the states generated by a multiport beam splitter. We consider three paradigmatic scenarios according to the input state: (a) input states that are finite superpositions of number states, (b) input states that are finite superpositions of coherent states, and (c) input states that are finite superpositions of both number and coherent states. This restriction to finite superpositions comes from the observations in Ref. [21], where it is shown that even in the bipartite case there exist states with an infinite degree of entanglement that cannot be connected through SLOCC. We show that the multipartite entanglement classes of scenario (a) are governed by a hierarchy based on the highest total number of photons in the state, while the classes in scenario (b) follow a hierarchy based on the so-called nonclassicality rank [17,18]. Interestingly, some superpositions of qudit Dicke states [22–24] and a recent generalization of these [25] fall in the classification scheme of scenario (a). In Sec. IV, we compare the three types of states arising from scenarios (a), (b), and (c), showing that each scenario constitutes a multipartite entanglement class of its own and that this induces inequivalencies between the corresponding input states. Finally in Sec. V, we discuss the conclusions of the results as well as perspectives on future problems.

II. PRELIMINARIES

A. Multipartite entanglement classes

We consider a state space $\mathcal{H}$ composed of m subsystems $\mathcal{H}_1, \mathcal{H}_2, \dots, \mathcal{H}_m$, i.e., $\mathcal{H} = \bigotimes_{k=1}^m \mathcal{H}_k$. Let $\dim(\mathcal{H}_k) = d_k$ and let $\{|e_1, e_2, \dots, e_m\rangle\}$ denote the computational basis of $\mathcal{H}$, with $e_k = 0, 1, \dots, d_k - 1$. An arbitrary state $|\Psi\rangle \in \mathcal{H}$ is written in the computational basis as

$$|\Psi\rangle = \sum_{e_k=0}^{d_k-1} \Psi_{e_1e_2\dots e_m}|e_1, e_2, \dots, e_m\rangle,$$

where the scalars $\Psi_{e_1e_2\dots e_m}$ constitute the so-called coefficient tensor of the state $|\Psi\rangle$. For the purposes of this work, we can assume $d_1 = d_2 = \dots = d_m = d$. We can arrange the coefficients $\Psi_{e_1e_2\dots e_m}$ in a matrix $\mathcal{M}_{|\Psi\rangle} = (\Psi_{e_1,e_2\dots e_m})$, called the coefficient matrix of $|\Psi\rangle$, where the rows are indexed by the values $e_1 = 0, 1, \dots, d-1$, while the columns are indexed by the remaining values $e_2 \dots e_m$ in lexicographic order. We can then arrange $\mathcal{M}_{|\Psi\rangle}$ as

$$\mathcal{M}_{|\Psi\rangle} = (M_0|M_1|\dots|M_{d^{m-2}-1}),$$

[*]Contact author: steinhofffrank@gmail.com

where each submatrix M_k is a $d\times d$ block. For the bipartite case $m = 2$, the coefficient matrix is a proper matrix:

$$\mathcal{M}_{|\Psi\rangle} = \begin{pmatrix} \Psi_{0,0} & \Psi_{0,1} & \dots & \Psi_{0,d-1} \\ \Psi_{1,0} & \Psi_{1,1} & \dots & \Psi_{1,d-1} \\ \vdots & \vdots & & \vdots \\ \Psi_{d-1,0} & \Psi_{d-1,1} & \dots & \Psi_{d-1,d-1} \end{pmatrix}.$$

The coefficient matrix for the case $d = 2$ and $m = 3$ (three qubits) is given by

$$\mathcal{M}_{|\Psi\rangle} = \left(\begin{array}{cc|cc} \Psi_{0,00} & \Psi_{0,01} & \Psi_{0,10} & \Psi_{0,11} \\ \Psi_{1,00} & \Psi_{1,01} & \Psi_{1,10} & \Psi_{1,11} \end{array}\right).$$

In general, we say that a state ρ is SLOCC equivalent to ρ' (notation: $\rho \sim \rho'$) if one can be obtained from the other by the sole use of SLOCC procedures; otherwise, we call the states SLOCC inequivalent. For pure states, the problem simplifies significantly [2].

Observation 1. The m-partite pure states $|\Psi\rangle$ and $|\Phi\rangle$ are SLOCC equivalent if and only if there exists invertible local operators (ILOs) L_k such that

$$|\Phi\rangle = L_1 \otimes L_2 \otimes \cdots \otimes L_m|\Psi\rangle.$$

Besides entanglement, ILOs play an important role in hidden nonlocality [26,27], where they are known as local filters. The action of ILOs on a state $|\Psi\rangle$ induces linear operations on the rows and columns of the coefficient matrix $\mathcal{M}_{|\Psi\rangle}$. For the bipartite case $m = 2$, the rank of $\mathcal{M}_{|\Psi\rangle}$, called the Schmidt rank of $|\Psi\rangle$, is invariant under ILOs and thus two bipartite pure states are SLOCC equivalent if and only if they have the same (finite) Schmidt rank [14,28]. For $m > 3$, we say that a state is genuinely mutipartite entangled if it is entangled with respect to any bipartition of the state space, i.e., if the Schmidt rank of any bipartition is greater than 1.

The three-qubit case $d = 2$ and $m = 3$ reveals that there are two SLOCC-inequivalent classes of genuinely entangled states [8]: the Greenberger-Home-Zeilinger (GHZ) class, with representative $|\text{GHZ}\rangle = 2^{-1/2}(|000\rangle + |111\rangle)$ and the W class, with representative $|W\rangle = 3^{-1/2}(|001\rangle + |010\rangle + |100\rangle)$. For the four-qubit case $d = 2$ and $m = 4$, it is known that there exists an infinite number of SLOCC-inequivalent genuinely entangled states and it is then more practical to classify states in terms of a finite number of families of SLOCC-equivalent classes [10].

For the construction of some of the ILOs connecting SLOCC-equivalent states, we use the ideas of Ref. [14], where ILOs are decomposed as finite sequences of elementary local operations (ELOs). It is possible to then employ a multipartite version of the Gauss-Jordan elimination procedure on the coefficient matrix of a state in order to map it into the coefficient matrix of a suitable state that is representative of this class. Other multipartite entanglement classification schemes based on the coefficient matrix are found in Refs. [11,12,29–31].

B. States generated by a multiport beam splitter

A MBS is an optical device that implements linear operations on the creation and annihilation operators on m spatial modes [32]. Specifically, if we write a vector $\mathbf{a}^\dagger = (a_1^\dagger, a_2^\dagger, \dots, a_m^\dagger)$, then the effect of the MBS is to perform the map $\mathbf{a}^\dagger \to S\mathbf{a}^\dagger$, where S, the so-called scattering matrix, is an element of $\mathcal{SU}(m)$; a similar transformation takes place for the annihilation operators. Alternatively, one can see the effect of the MBS as the unitary action $a_k^\dagger \to U_S a_k^\dagger U_S^\dagger$, for $k = 1, \dots, m$.

We are mainly interested in input states of the form $|\psi\rangle \otimes |0, 0, \dots, 0\rangle$, where all modes but the first one are equal to the vacuum state. The reason for this restriction is to avoid interference effects between different modes, which can complicate considerably the problem of entanglement classification [33–35]. Moreover, the MBS is a passive physical device and any quantum correlation present at its exit can be traced back to the quantum correlations of the single-mode state $|\psi\rangle$ entering the MBS [17–20]. With this restriction in mind, we show in Appendix A that a balanced MBS on the first mode, in the sense that

$$a_1^\dagger \to U_S a_1^\dagger U_S^\dagger = \frac{a_1^\dagger + a_2^\dagger + \dots + a_m^\dagger}{\sqrt{m}},$$

is sufficient for the SLOCC classification of output states of any MBS; thus, without loss of generality, in what follows we only consider the action of a balanced MBS.

A number state on the first mode is given by

$$|n, 0, \dots, 0\rangle = \frac{(a_1^\dagger)^n}{\sqrt{n!}}|0, 0, \dots, 0\rangle.$$

The output state of the MBS $|\Psi_n\rangle = U_S|n, 0, \dots, 0\rangle$ is thus

$$\begin{aligned} |\Psi_n\rangle &= \frac{1}{\sqrt{n!}}\left(\frac{a_1^\dagger + a_2^\dagger + \dots + a_m^\dagger}{\sqrt{m}}\right)^n |0, 0, \dots, 0\rangle \\ &= \sum_{n_1+\dots+n_m=n} \binom{n}{n_1, \dots, n_m} \frac{(a_1^\dagger)^{n_1} \dots (a_m^\dagger)^{n_m}}{\sqrt{n! m^n}} |0, \dots, 0\rangle, \end{aligned}$$

where the summation runs through all the possible non-negative integer values $n_1, \dots, n_m$ satisfying the constraint $n_1 + \dots + n_m = n$ and we use the multinomial coefficient

$$\binom{n}{n_1, \dots, n_m} = \frac{n!}{n_1! n_2! \dots n_m!}.$$

Some simple algebraic manipulation results in

$$|\Psi_n\rangle = \frac{1}{m^{n/2}} \sum_{n_1+\dots+n_m=n} \sqrt{\binom{n}{n_1, \dots, n_m}} |n_1 \dots n_m\rangle.$$

This state is symmetrical with respect to any permutation of the modes.

Another interesting type of input state is the coherent state

$$|\alpha, 0, \dots, 0\rangle = D_1(\alpha)|0, 0, \dots, 0\rangle,$$

where $D_1(\alpha) = e^{\alpha a_1^\dagger - \alpha^* a_1}$ is the displacement operator. The output state $U_S|\alpha, 0, \dots, 0\rangle$ then reads

$$|\eta_\alpha\rangle = |\alpha/\sqrt{m}, \alpha/\sqrt{m}, \dots, \alpha/\sqrt{m}\rangle,$$

since $U_S D_1(\alpha) U_S^\dagger = D_1(\alpha/\sqrt{m}) D_2(\alpha/\sqrt{m}) \dots D_m(\alpha/\sqrt{m})$.

III. RESULTS

A. Superpositions of number states as input

We consider an m-port balanced beam splitter and an input state on the first mode given by

$$|\psi\rangle \otimes |0,\dots,0\rangle = \sum_{n=0}^{N} c_n |n,0,\dots,0\rangle,$$

representing an arbitrary finite superposition of number states. The value N represents the highest total number of photons or energy. A finite superposition of number states can be obtained from an infinite one via truncation methods [36–38]. The resulting output state of the MBS is then

$$|\Psi\rangle = U_S|\psi\rangle \otimes |0,\dots,0\rangle = \sum_{n=0}^{N} c_n|\Psi_n\rangle, \tag{1}$$

where, according to the previous section,

$$|\Psi_n\rangle = \sum_{n_1+\dots+n_m=n} C^n_{n_1\dots n_m}|n_1\dots n_m\rangle;$$

$$C^n_{n_1\dots n_m} = \frac{1}{m^{n/2}}\sqrt{\binom{n}{n_1,\dots,n_m}}. \tag{2}$$

We now show that $|\Psi\rangle$ can be brought to a more convenient form $|\Phi\rangle = \sum_{n=0}^{N} h_n|\Phi_n\rangle$, where $h_n = c_n\sqrt{\frac{n!}{m^n}}$ and we define the un-normalized states[1]

$$|\Phi_n\rangle = \sum_{n_1+\dots+n_m=n} |n_1\dots n_m\rangle,$$

which we call uniform states. Some superpositions of these uniform states were considered in Ref. [14], based on the related work [39] and having interesting properties such as coefficient matrices with special structures. Moreover, some of the so-called qudit Dicke states [22–24], as well as the recent spin-s Dicke states [25], can be seen as specific superpositions of the uniform states $|\Phi_n\rangle$, i.e., are special cases of states in the form $|\Phi\rangle = \sum_{n=0}^{N} h_n|\Phi_n\rangle$ and hence their SLOCC classification can be obtained within our framework.

Observation 2. The output state $|\Psi\rangle$ is SLOCC equivalent to $|\Phi\rangle$. In particular, $|\Psi_n\rangle \sim |\Phi_n\rangle$ for any value of n.

Proof. Given the following invertible operation on mode k,

$$R_k = \sum_{n_k=0}^{N} \sqrt{n_k!}|n_k\rangle\langle n_k|,$$

we notice first that

$$\begin{aligned}\bigotimes_{k=1}^{m} R_k|\Psi_n\rangle &= \sum_{n_1+\dots+n_m=n} C^n_{n_1\dots n_m}\bigotimes_{k=1}^{m} R_k|n_1\dots n_m\rangle\\ &= \sum_{n_1+\dots+n_m=n} C^n_{n_1\dots n_m}\sqrt{n_1!\dots n_m!}|n_1\dots n_m\rangle\\ &= \sqrt{\frac{n!}{m^n}}\sum_{n_1+\dots+n_m=n}|n_1\dots n_m\rangle = \sqrt{\frac{n!}{m^n}}|\Phi_n\rangle.\end{aligned}$$

We thus conclude that

$$\bigotimes_{k=1}^{m} R_k|\Psi\rangle = \sum_{n=0}^{N} c_n \bigotimes_{k=1}^{m} R_k|\Psi_n\rangle = \sum_{n=0}^{N} h_n|\Phi_n\rangle = |\Phi\rangle,$$

where $h_n = c_n\sqrt{\frac{n!}{m^n}}$. ■

We are now ready to show that the output state $|\Psi\rangle = \sum_{n=0}^{N} c_n|\Psi_n\rangle$ is SLOCC equivalent to $|\Psi_N\rangle$, i.e., the term with highest number of photons.

Observation 3. The uniform state $|\Phi\rangle$ is SLOCC equivalent to $|\Phi_N\rangle$. Moreover, we have the following chain of SLOCC equivalences:

$$|\Psi\rangle \sim |\Phi\rangle \sim |\Phi_N\rangle \sim |\Psi_N\rangle.$$

Proof. In what follows, $\overline{x}$ denotes the number $x/(N+1)$ in base $N+1$. For example, if $N=3$, then $\overline{56} = 32$, since $56/4 = 14$ and 14 equals $32 = 3.4^1 + 2.4^0$ in base 4. The state $|\Phi\rangle$ has a coefficient matrix given by $\mathcal{M}_{|\Phi\rangle} = (\Phi_{n_1,n_2\dots n_m})$. We then write the array $n_2\dots n_m$, which gives the columns of $\mathcal{M}_{|\Phi\rangle}$, as $\overline{n_2\dots n_m}$. The coefficient matrix of $|\Phi\rangle$ can then be written as

$$\mathcal{M}_{|\Psi\rangle} = \left(M_{\overline{0}}|M_{\overline{1}}|M_{\overline{2}}|\dots|M_{\overline{d^{m-2}-1}}\right),$$

where the submatrices $M_{\overline{k}}$ are indexed according to their first column k with the decimal expression $n_2n_3\dots n_m$; notice that k is then a multiple of $N+1$. This notation is to take into account the repetitions of submatrices that occur for $m>3$, as well as identifying null submatrices and allowing possible future generalizations for the infinite superposition case. Moreover, let $||\vec{k}|| = n_2 + n_3 + \dots + n_m$. The submatrices $M_{\overline{k}}$ are Hankel matrices [40] of a special form,

$$M_{\overline{0}} = \begin{pmatrix} h_0 & h_1 & h_2 & h_3 & \dots & h_N\\ h_1 & h_2 & h_3 & \dots & h_N & 0\\ h_2 & h_3 & & \iddots & 0 & \vdots\\ h_3 & \vdots & \iddots & \iddots & & \\ \vdots & h_N & 0 & & & \vdots\\ h_N & 0 & \dots & & \dots & 0\end{pmatrix},$$

$$M_{\overline{k}} = \left(\begin{array}{cccccc|c} h_1 & h_2 & h_3 & h_4 & \dots & h_N & 0\\ h_2 & h_3 & h_4 & \dots & h_N & 0 & 0\\ h_3 & h_4 & & \iddots & 0 & \vdots & \vdots\\ h_4 & \vdots & \iddots & \iddots & & & \vdots\\ \vdots & h_N & 0 & & & \vdots & 0\\ h_N & 0 & \dots & & \dots & 0 & 0\\ \hline 0 & 0 & \dots & & \dots & 0 & 0\end{array}\right),$$

$||\vec{k}|| = 1$,

$$M_{\overline{k}} = \left(\begin{array}{cccccc|cc} h_2 & h_3 & h_4 & h_5 & \dots & h_N & 0 & 0\\ h_3 & h_4 & h_5 & \dots & h_N & 0 & 0 & 0\\ h_4 & h_5 & & \iddots & 0 & \vdots & \vdots & \vdots\\ h_5 & \vdots & \iddots & \iddots & & & \vdots & \vdots\\ \vdots & h_N & 0 & & & \vdots & 0 & 0\\ h_N & 0 & \dots & & \dots & 0 & 0 & 0\\ \hline 0 & 0 & \dots & & \dots & 0 & 0 & 0\\ 0 & 0 & \dots & & \dots & 0 & 0 & 0\end{array}\right),$$

$||\vec{k}|| = 2$,

[1]An un-normalized state $|\nu\rangle$ is trivially SLOCC equivalent to its normalized version via the ILO $\frac{1}{\sqrt{\langle\nu|\nu\rangle}}\mathcal{I}$.

and an arbitrary submatrix with $||\vec{k}|| = n$ is given by

$$M_{\vec{k}} = \left(\begin{array}{cccccc|ccc} h_n & h_{n+1} & h_{n+2} & h_{n+3} & \dots & h_N & 0 & \dots & 0 \\ h_{n+1} & h_{n+2} & h_{n+3} & \dots & h_N & 0 & 0 & \dots & 0 \\ h_{n+2} & h_{n+3} & & \iddots & 0 & \vdots & \vdots & & \vdots \\ h_{n+3} & \vdots & \iddots & \iddots & & & & & \\ \vdots & h_N & 0 & & & \vdots & \vdots & & \vdots \\ h_N & 0 & \dots & & \dots & 0 & 0 & \dots & 0 \\ \hline 0 & 0 & \dots & & \dots & 0 & 0 & \dots & 0 \\ \vdots & \vdots & & & & \vdots & \vdots & & \vdots \\ 0 & 0 & \dots & & \dots & 0 & 0 & \dots & 0 \end{array}\right).$$

Notice that if $||\vec{k}|| > N$, the submatrix $M_{\vec{k}}$ is a null matrix. Let $A = A^{(N-1)}A^{(N-2)}\dots A^{(1)}A^{(0)}$, where $A^{(k)} = \mathcal{I} + \sum_{n=k}^{N-1} \lambda_n |n\rangle\langle N-k|$, with $\mathcal{I}$ denoting the identity operator and $\lambda_n = -h_n/h_N$. The matrices representing these operators in the number basis are given by

$$A^{(0)} = \begin{pmatrix} 1 & & & & \lambda_0 \\ & 1 & & & \lambda_1 \\ & & \ddots & & \vdots \\ & & & 1 & \lambda_{N-1} \\ & & & & 1 \end{pmatrix},$$

$$A^{(1)} = \begin{pmatrix} 1 & & & & \lambda_1 & \\ & 1 & & & \lambda_2 & \\ & & \ddots & & \vdots & \\ & & & 1 & \lambda_{N-1} & \\ & & & & 1 & \\ & & & & & 1 \end{pmatrix},$$

and, in general,

$$A^{(k)} = \begin{pmatrix} 1 & & & & \lambda_k & & & \\ & 1 & & & \lambda_{k+1} & & & \\ & & \ddots & & \vdots & & & \\ & & & 1 & \lambda_{N-1} & & & \\ & & & & 1 & & & \\ & & & & & \ddots & & \\ & & & & & & 1 & \\ & & & & & & & 1 \end{pmatrix}, \quad k = 0, 1, \dots, N-1,$$

where the empty spaces are to be understood as 0. Notice that each $A^{(k)}$ is the product of ELOs that implement Gaussian elimination on the lines of the coefficient matrix [14].

Let A_q denote the operator A just introduced acting on mode q. The operation $A_1|\Phi\rangle = A_1^{(N-1)}A_1^{(N-2)}\dots A_1^{(1)}A_1^{(0)}|\Phi\rangle$ corresponds to the left multiplication $AM_{\vec{k}}$ of each submatrix of the coefficient matrix. The operation $A_1^{(0)}|\Phi\rangle$ amounts to mapping $M_{\vec{0}}$ into

$$A^{(0)}M_{\vec{0}} = \begin{pmatrix} 0 & h_1 & h_2 & h_3 & \dots & h_N \\ 0 & h_2 & h_3 & \dots & h_N & 0 \\ \vdots & h_3 & \vdots & \iddots & 0 & \vdots \\ \vdots & \vdots & h_N & \iddots & & \\ 0 & h_N & 0 & & & \vdots \\ h_N & 0 & \dots & & \dots & 0 \end{pmatrix},$$

while the other submatrices are unchanged. The operation $A_1^{(1)}A_1^{(0)}|\Phi\rangle$ maps $A^{(0)}M_{\vec{0}}$ into

$$A^{(1)}A^{(0)}M_{\vec{0}} = \begin{pmatrix} 0 & 0 & h_2 & h_3 & \dots & h_N \\ 0 & 0 & h_3 & \dots & h_N & 0 \\ \vdots & \vdots & \vdots & \iddots & 0 & \vdots \\ \vdots & 0 & h_N & \iddots & & \\ 0 & h_N & 0 & & & \vdots \\ h_N & 0 & \dots & & \dots & 0 \end{pmatrix},$$

while the various $M_{\vec{k}}$ with $||\vec{k}|| = 1$ are mapped into

$$A^{(1)}M_{\vec{k}} = \left(\begin{array}{cccccc|c} 0 & h_2 & h_3 & h_4 & \dots & h_N & 0 \\ 0 & h_3 & h_4 & \dots & h_N & 0 & 0 \\ 0 & h_4 & \vdots & \iddots & 0 & \vdots & \vdots \\ \vdots & \vdots & h_N & \iddots & & & \vdots \\ 0 & h_N & 0 & & & \vdots & 0 \\ h_N & 0 & \dots & & \dots & 0 & 0 \\ \hline 0 & 0 & \dots & & \dots & 0 & 0 \end{array}\right)$$

and the other submatrices are unchanged. The operation $A_1^{(2)}A_1^{(1)}A_1^{(0)}|\Phi\rangle$ maps $A^{(1)}A^{(0)}M_{\vec{0}}$ into

$$A^{(2)}A^{(1)}A^{(0)}M_{\vec{0}} = \begin{pmatrix} 0 & 0 & 0 & h_3 & h_4 & \dots & h_N \\ 0 & 0 & 0 & h_4 & \dots & h_N & 0 \\ \vdots & \vdots & \vdots & \vdots & \iddots & 0 & 0 \\ \vdots & \vdots & 0 & h_N & \iddots & 0 & \vdots \\ \vdots & 0 & h_N & 0 & \iddots & & \\ 0 & h_N & 0 & 0 & & & \vdots \\ h_N & 0 & 0 & \dots & & \dots & 0 \end{pmatrix},$$

maps the various $A^{(1)}M_{\vec{k}}$ with $||\vec{k}|| = 1$ into

$$A^{(2)}A^{(1)}M_{\vec{k}} = \left(\begin{array}{cccccc|c} 0 & 0 & h_3 & h_4 & \dots & h_N & 0 \\ 0 & 0 & h_4 & \dots & h_N & 0 & 0 \\ 0 & \vdots & \vdots & \iddots & 0 & \vdots & \vdots \\ \vdots & 0 & h_N & \iddots & & & \\ 0 & h_N & 0 & & & \vdots & \vdots \\ h_N & 0 & \dots & & \dots & 0 & 0 \\ \hline 0 & 0 & \dots & & \dots & 0 & 0 \end{array}\right)$$

and the various $M_{\vec{k}}$ with $||\vec{k}|| = 2$ into

$$A^{(2)}M_{\vec{k}} = \left(\begin{array}{cccccc|cc} 0 & h_3 & h_4 & h_5 & \dots & h_N & 0 & 0 \\ 0 & h_4 & h_5 & \dots & h_N & 0 & 0 & 0 \\ \vdots & h_5 & \vdots & \iddots & 0 & \vdots & \vdots & \vdots \\ \vdots & \vdots & h_N & \iddots & & & \vdots & \vdots \\ 0 & h_N & 0 & & & \vdots & 0 & 0 \\ h_N & 0 & \dots & & \dots & 0 & 0 & 0 \\ \hline 0 & 0 & \dots & & \dots & 0 & 0 & 0 \\ 0 & 0 & \dots & & \dots & 0 & 0 & 0 \end{array}\right),$$

while the other submatrices are unchanged. It is easy to see then that the overall effect of $A_1|\Phi\rangle$ on the various submatrices such that $||\vec{k}|| = n$ is

$$M_{\vec{k}} \rightarrow \left(\begin{array}{cccccc|ccc} 0 & 0 & \dots & 0 & 0 & h_N & 0 & \dots & 0 \\ 0 & 0 & \dots & 0 & h_N & 0 & 0 & \dots & 0 \\ 0 & \vdots & & \iddots & 0 & \vdots & \vdots & & \vdots \\ \vdots & 0 & \iddots & \iddots & & & & & \\ 0 & h_N & 0 & & & \vdots & \vdots & & \vdots \\ h_N & 0 & \dots & & \dots & 0 & 0 & \dots & 0 \\ \hline 0 & 0 & \dots & & \dots & 0 & 0 & \dots & 0 \\ \vdots & \vdots & & & & \vdots & \vdots & & \vdots \\ 0 & 0 & \dots & & \dots & 0 & 0 & \dots & 0 \end{array}\right).$$

Defining $Y = (1/h_N)\mathcal{I}$, we see that $YA_1|\Phi\rangle = |\Phi_N\rangle$. ■

In Appendix B, we use Observation 3 to show that the Schmidt rank of $|\Psi\rangle$ for any bipartition of the modes is $N + 1$, implying that it is a genuinely m-partite entangled state if $N \neq 0$. Since the Schmidt rank is invariant under SLOCC, we see that $|\Psi_n\rangle$ and $|\Psi_{n'}\rangle$ are SLOCC inequivalent whenever $n \neq n'$. In other words, for each value of n there is a SLOCC equivalence class $\mathcal{C}_n$ with representatives $|\Psi_n\rangle$ and $|\Phi_n\rangle$. The set $\mathcal{C}_n$ is convex, with mixed states comprised of convex combinations of the pure states in this SLOCC equivalence class; for a mixed state with the density matrix ρ, the minimum Schmidt rank of the pure states that are needed to construct ρ is called the Schmidt number of ρ [41,42].

Moreover, the Schmidt number implies the following hierarchy among the SLOCC classes [43], as depicted in Fig. 1:

$$\mathcal{C}_0 \subset \mathcal{C}_1 \subset \mathcal{C}_2 \subset \cdots \subset \mathcal{C}_{n-1} \subset \mathcal{C}_n \subset \mathcal{C}_{n+1} \subset \cdots.$$

Similarly to the relation between the GHZ and W classes [44], pure states in $\mathcal{C}_K$ are those SLOCC equivalent to $|\Psi_K\rangle$. By Observation 3, all states in the form

$$|\Psi\rangle = c_0|\Psi_0\rangle + c_1|\Psi_1\rangle + \cdots + c_K|\Psi_K\rangle$$

are in $\mathcal{C}_K$ as well. Hence, we can always find a $|\Psi\rangle \in \mathcal{C}_K$ that is arbitrarily close (but never equal) to $|\Psi_k\rangle$ if $k < K$, e.g., by

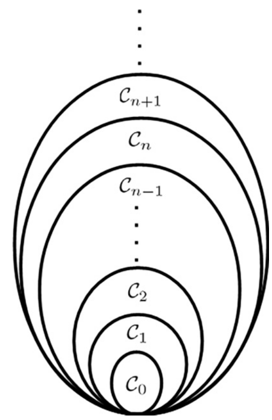

FIG. 1. Structure of SLOCC classes for input states that are finite superpositions of number states.

making $c_k \rightarrow 1$. The converse is not valid; however, since we cannot increase the Schmidt rank of any bipartition by ILOs, implying that it is not possible to find a state in $\mathcal{C}_K$ arbitrarily close to a given state in $\mathcal{C}_{K+1}$. This relation among the classes can be inferred as well from the maximum overlap between a given representative in a class and the whole set of states of some other class [45].

B. Superpositions of coherent states as input

We now consider arbitrary "cat states" [46] of the form

$$|\psi\rangle = \frac{1}{\mathcal{N}} \sum_{k=0}^{r-1} c_k|\alpha_k\rangle$$

on the first mode, where $|\alpha_k\rangle$ are distinct coherent states and $\mathcal{N}$ is a normalization factor. The number r represents the so-called nonclassicality rank [17,18] of the input state.

This finite superposition of coherent states, when going through an m-port beam splitter, results in the output state

$$|\Psi\rangle = U_S|\psi\rangle \otimes |0, \dots, 0\rangle = \frac{1}{\mathcal{N}} \sum_{k=0}^{r-1} c_k|\eta_{\alpha_k}\rangle,$$

where $|\eta_{\alpha_k}\rangle = |\beta_k, \dots, \beta_k\rangle$ and $\beta_k = \alpha_k/\sqrt{m}$.

Observation 4. The output state $|\Psi\rangle$ is SLOCC equivalent to the GHZ state

$$|\text{GHZ}_{(r)}\rangle = \frac{|0\rangle^{\otimes m} + |1\rangle^{\otimes m} + \cdots + |r-1\rangle^{\otimes m}}{\sqrt{r}}.$$

Proof. In each mode, the states $|\beta_0\rangle, |\beta_1\rangle, \dots, |\beta_{r-1}\rangle$ form a linearly independent set [47]. By Gram-Schmidt orthogonalization [48], there exists an invertible operator B such that the states $|\chi_k\rangle = B|\beta_k\rangle$, $k = 0, 1, \dots, r-1$, form an orthonormal basis. Moreover, the unitary $W = \sum_{k=0}^{r-1} |k\rangle\langle\chi_k|$ changes from the $\{|\chi_0\rangle, |\chi_1\rangle, \dots, |\chi_{r-1}\rangle\}$ basis to the number basis $\{|0\rangle, |1\rangle, \dots, |r-1\rangle\}$. Defining $T = \sum_{n=0}^{r-1} c_n^{-1}|n\rangle\langle n|$ and $Y' = (\mathcal{N}/\sqrt{r})\mathcal{I}$, we have

$$Y'T_1 \bigotimes_{q=1}^{m} W_q B_q|\Psi\rangle = \frac{1}{\sqrt{r}} \sum_{k=0}^{r-1} |k, k, \dots, k\rangle,$$

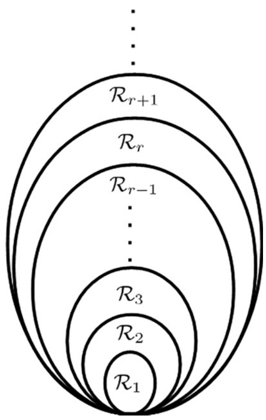

FIG. 2. Structure of SLOCC classes for input states that are finite superpositions of coherent states.

and we have shown that $|\Psi\rangle$ is SLOCC equivalent to the m-partite GHZ state $|\mathrm{GHZ}_{(r)}\rangle$. ■

With a reasoning similar to the previous case, each state $|\mathrm{GHZ}_{(r)}\rangle$ constitutes a representative of a SLOCC equivalence class $\mathcal{R}_r$, $(r = 1, 2\ldots)$. The Schmidt rank of $|\mathrm{GHZ}_{(r)}\rangle$ for any bipartition of the state space $\mathcal{H}$ is obviously r. We deduce then a hierarchy based on the nonclassicality rank of the input state, as depicted in Fig. 2:

$$\mathcal{R}_1 \subset \mathcal{R}_2 \subset \mathcal{R}_3 \subset \cdots \subset \mathcal{R}_{r-1} \subset \mathcal{R}_r \subset \mathcal{R}_{r+1} \subset \cdots .$$

Let $C = \sum_{n=0}^{r-1} d_n |n\rangle\langle n|$. Then we have

$$C_1|\mathrm{GHZ}_{(r)}\rangle = \frac{1}{\sqrt{r}} \sum_{k=0}^{r-1} d_k |k, k, \ldots, k\rangle.$$

It is clear then that $|\mathrm{GHZ}_{(r)}\rangle$ can be made arbitrarily close to $|\mathrm{GHZ}_{(r')}\rangle$ for $r' < r$, but the converse is not true for $r' > r$.

C. Hybrid superpositions

A more exotic example of the input state is a finite superposition of both number and coherent states,

$$|\psi\rangle = \frac{1}{\mathcal{N}} \left(\sum_{n=0}^{N} c_n |n\rangle + \sum_{k=0}^{r-1} d_k |\alpha_k\rangle \right),$$

where $\mathcal{N}$ stands for a normalization factor. The output state produced by a MBS when $|\psi\rangle$ is the input is, according to the previous discussion,

$$|\Psi\rangle = \frac{1}{\mathcal{N}} \left(\sum_{n=0}^{N} c_n |\Psi_n\rangle + \sum_{k=0}^{r-1} d_k |\eta_{\alpha_k}\rangle \right),$$

where $|\eta_{\alpha_k}\rangle = |\beta_k, \ldots, \beta_k\rangle$ and $\beta_k = \alpha_k/\sqrt{m}$.

Observation 5. The output state $|\Psi\rangle$ is SLOCC equivalent to the state

$$|\Phi_N\rangle + \sum_{n=N+1}^{N+r} |n\rangle^{\otimes m}.$$

Proof. The set of states $\{|0\rangle, |1\rangle, \ldots, |N\rangle\} \cup \{|\beta_0\rangle, |\beta_1\rangle, \ldots, |\beta_{r-1}\rangle\}$ is linearly independent in each mode. By Gram-Schmidt orthogonalization [48], there exists an invertible operator F such that $F|n\rangle = |n\rangle$, $n = 0, 1, \ldots, N$, and $|\mu_k\rangle = F|\beta_k\rangle$, $k = 0, 1, \ldots, r-1$, and such that $\{|0\rangle, |1\rangle, \ldots, |N\rangle\} \cup \{|\mu_0\rangle, |\mu_1\rangle, \ldots, |\mu_{r-1}\rangle\}$ forms an orthonormal basis. The unitary $V = \sum_{n=0}^{N} |n\rangle\langle n| + \sum_{k=N+1}^{N+r} |k\rangle\langle \mu_{k-(N+1)}|$ changes from the $\{|0\rangle, |1\rangle, \ldots, |N\rangle\} \cup \{|\mu_0\rangle, |\mu_1\rangle, \ldots, |\mu_{r-1}\rangle\}$ basis to the number basis $\{|0\rangle, |1\rangle, \ldots, |N\rangle, |N+1\rangle, |N+2\rangle, \ldots, |N+r\rangle\}$. Defining $Q = \sum_{n=0}^{N} |n\rangle\langle n| + \sum_{n=N+1}^{N+r} d_n^{-1} |n\rangle\langle n|$ and $P = (\mathcal{N})\mathcal{I}$, we have

$$Q_1 P_1 \bigotimes_{q=1}^{m} V_q F_q |\Psi\rangle = \sum_{n=0}^{N} c_n |\Psi_n\rangle + \sum_{n=N+1}^{N+r} |n\rangle^{\otimes m}.$$

Let $G = \sum_{n=0}^{N} \sqrt{n!} |n\rangle\langle n| + \sum_{n=N+1}^{N+r} |n\rangle\langle n|$; we have, according to the proof of Observation 2,

$$\bigotimes_{q=1}^{m} G_q \left(\sum_{n=0}^{N} c_n |\Psi_n\rangle + \sum_{n=N+1}^{N+r} |n\rangle^{\otimes m} \right) = \sum_{n=0}^{N} h_n |\Phi_n\rangle + \sum_{n=N+1}^{N+r} |n\rangle^{\otimes m}.$$

Let A and Y be the operators used in the proof of Observation 3. Then we have

$$Y A_1 \left(\sum_{n=0}^{N} h_n |\Phi_n\rangle + \sum_{n=N+1}^{N+r} |n\rangle^{\otimes m} \right) = |\Phi_N\rangle + \sum_{n=N+1}^{N+r} |n\rangle^{\otimes m},$$

and the output state $|\Psi\rangle$ is thus SLOCC equivalent to $|\Phi_N\rangle + \sum_{n=N+1}^{N+r} |n\rangle^{\otimes m}$. ■

By previous results, the Schmidt rank of $|\Phi_N\rangle + \sum_{n=N+1}^{N+r} |n\rangle^{\otimes m}$ is $N + r + 1$. Hence, there are different values of N and r where the respective states states have equal Schmidt ranks. For example, the states $|\Phi_3\rangle + \sum_{n=4}^{5} |n\rangle^{\otimes m}$ and $|\Phi_2\rangle + \sum_{n=3}^{5} |n\rangle^{\otimes m}$ both have Schmidt rank 6. As discussed in the next session, these states are SLOCC inequivalent, despite having equal Schmidt ranks.

IV. COMPARISON BETWEEN THE THREE SCENARIOS

We considered the three types of superpositions of the previous section separately and, in order to determine whether each type of representative is equivalent or inequivalent under SLOCC, we invoke the following result from Refs. [49,50].

Theorem 1. Two pure states of a multipartite system are equivalent under SLOCC if and only if (i) they have the same local rank of each party, and (ii) the ranges of the adjoint reduced density matrices of each party of them are related by certain ILOs.

By adjoint reduced density matrices, we can understand the density matrices obtained through discarding (partial trace) of one of the local subsystems $\mathcal{H}_k$ of the global system $\mathcal{H} = \mathcal{H}_1 \otimes \mathcal{H}_2 \otimes \cdots \otimes \mathcal{H}_m$. Denoting by a_k the number of product states in the range of the adjoint reduced density matrix related to $\mathcal{H}_k$, it is a consequence of Theorem 1 above that, if two states are SLOCC equivalent, then the array of values $[a_1, a_2, \ldots, a_m]$ of these states must be equal. Or, equivalently, if any value a_k differs for these states, then they are SLOCC inequivalent.

Due to the full permutational symmetry of the states considered and the simple form of the representatives in each scenario, the values a_k of a given state are all equal and are easily obtained. Following the notation in Refs. [49,50], we have the following classification:

(i) $|\Psi_N\rangle \sim |\Phi_N\rangle \in [1, 1, \dots, 1]$.

(ii) $|\mathrm{GHZ}_{(r)}\rangle \in [r, r, \dots, r]$.

(iii) $|\Phi_N\rangle + \sum_{n=N+1}^{N+r} |n\rangle^{\otimes m} \in [r+1, r+1, \dots, r+1]$.

It is straightforward then that each representative is SLOCC inequivalent to the other, even if they have the same Schmidt rank. For example, the Schmidt rank of $|\mathrm{GHZ}_{(M)}\rangle$, $|\Psi_{M-1}\rangle$, and $|\Phi_{M-2}\rangle + |M-1\rangle^{\otimes m}$ is M, but each is respectively in $[M, M, \dots, M]$, $[1, 1, \dots, 1]$, and $[2, 2, \dots, 2]$, being thus inequivalent by SLOCC.

The inequivalence between the three scenarios does not imply a hierarchy among the different SLOCC classes. However, in the multiqubit situation there are analytical results concerning the relationship between the multiqubit GHZ and W classes [44,45], coming from parametrizations of the symmetric subspaces of multiqubits. The hierarchies between the SLOCC classes described here will thus remain an open question.

As shown in Refs. [17–20] the multipartite entanglement of the output state of a MBS is due to the nonclassicality of the single-mode input state. We see that, despite having the same Schmidt rank, the output states in each of the three scenarios just described belong to different SLOCC classes. Since there is a one-to-one correspondence between the Schmidt rank of the output state and the nonclassicality rank of the input state, this implies that *the input states are inequivalent, despite having equal nonclassicality ranks.* By inequivalent we mean that these input states could not be mapped into one another via single-mode classical operations, i.e., quantum operations that preserve the linearity in a and $a^\dagger$ [51]. For example, the input states $|1\rangle$ and $|\alpha\rangle + |\beta\rangle$ entering an m-port beam splitter result in output states in the m-partite SLOCC classes W and GHZ, respectively, as shown previously. Hence, $|1\rangle$ and $|\alpha\rangle + |\beta\rangle$ are inequivalent by single-mode classical operations.

V. CONCLUSIONS AND PERSPECTIVES

In this paper, we investigated the different multipartite entanglement classes that arise in a multiport beam splitter in three distinct situations, depending on the single-mode states that enter the device. In the first scenario, we considered input states that are finite superpositions of number states and concluded that the different SLOCC equivalence classes were related to the highest total number of the output state. Physically, this is the highest energy attained by the state and thus more energy results in more "powerful" multipartite entanglement. In the second scenario, we analyzed input states that are finite superpositions of coherent states and identified a hierarchy among the SLOCC classes, but this time in terms of the nonclassicality rank of the input state. In the third scenario, we considered a hybrid situation where the input states are a superposition of both number and coherent states, obtaining a SLOCC classification that is a combination of the other two scenarios. The multipartite entanglement classes corresponding to each scenario were all shown to be inequivalent to each other.

The results obtained here give possible alternatives for the generation of target multipartite entangled states with desirable properties. In regards to entanglement properties related to the SLOCC equivalence class of a state, our work shows that one could employ as an input a finite superposition of number states—which can be obtained by truncation of a suitable continuous-variable state [36]—in a given experimental scenario that favors this kind of preparation procedure, instead of using a number state itself, whose implementation can be challenging in various situations; see, however, Refs. [52,53] for recent proposals on efficient number state generation. Likewise, instead of directly generating a GHZ-like state [15,16,54], by using cat states as inputs on a MBS, one obtains a multipartite entangled state with the same SLOCC properties. Moreover, there are limitations to the manipulation of states via linear quantum-optical dynamics [35,55] and thus the possibility of finding alternative states within a desired SLOCC class should be studied.

For the classification of mixed states, one could employ the techniques in Refs. [44,45] in order to detect to which multipartite entanglement classes a given mixed output state belongs, besides the use of the Schmidt number [43]. A related problem is the physical implementation of so-called SLOCC witnesses in the quantum optical domain. These interesting and complex open questions go beyond the scope of the present work and will be investigated elsewhere.

ACKNOWLEDGMENTS

This work is part of institutional research projects from Universidade Federal de Mato Grosso: Projects No. 376/2020, "Characterization of quantum correlations," and No. 475/2023 "Mathematical aspects of quantum entanglement." The author acknowledges the technical support of the Wolfram Research team and is thankful to João Bosco de Siqueira for ideas and discussions.

APPENDIX

1. Generality of a balanced multiport beam splitter

We show here that a balanced MBS is sufficient for our classification scheme, i.e., the many different transmission and reflection terms in an unbalanced MBS do not influence the multipartite entanglement classification obtained, since these terms can be manipulated via the action of suitable ILOs on the final output state. In other words, the output state of an arbitrary unbalanced MBS will be shown to be SLOCC equivalent to the output state of a balanced MBS.

An arbitrary input state on the first mode is given by

$$|\psi\rangle = \sum_{n=0}^{\infty} c_n |n\rangle = \sum_{n=0}^{\infty} c_n \frac{(a_1^\dagger)^n}{\sqrt{n!}} |0\rangle.$$

If this state goes through an arbitrary unbalanced m-port beam splitter, the resulting output state is given by

$$\begin{aligned}|\tilde{\Psi}\rangle &= \sum_{n=0}^{\infty} \frac{c_n}{\sqrt{n!}} (\gamma_1 a_1^\dagger + \gamma_2 a_2^\dagger + \dots + \gamma_m a_m^\dagger)^n |0, 0, \dots, 0\rangle \\ &= \sum_{n=0}^{\infty} \frac{c_n}{\sqrt{n!}} \sum_{n_1+\dots+n_m=n} \binom{n}{n_1, n_2, \dots, n_m} (\gamma_1 a_1^\dagger)^{n_1} (\gamma_2 a_2^\dagger)^{n_2} \cdots (\gamma_m a_m^\dagger)^{n_m} |0, 0, \dots, 0\rangle \\ &= \sum_{n=0}^{\infty} c_n \sum_{n_1+\dots+n_m=n} \sqrt{\binom{n}{n_1, n_2, \dots, n_m}} \gamma_1^{n_1} \gamma_2^{n_2} \dots \gamma_m^{n_m} |n_1, n_2, \dots, n_m\rangle,\end{aligned}$$

where $\gamma_k \in \mathbb{C}$ and $|\gamma_1|^2 + |\gamma_2|^2 + \dots + |\gamma_m|^2 = 1$. Defining the following (bounded) ILO on mode q,

$$D_q = \frac{1}{\sqrt{m}} \sum_{q=0}^{\infty} (\gamma_q^{-1})^{n_q} |n_q\rangle\langle n_q|,$$

we see that its effect on the output state is

$$\begin{aligned}\bigotimes_{q=1}^{m} D_q |\tilde{\Psi}\rangle &= \sum_{n=0}^{\infty} c_n \sum_{n_1+\dots+n_m=n} \sqrt{\binom{n}{n_1, n_2, \dots, n_m}} \gamma_1^{n_1} \gamma_2^{n_2} \dots \gamma_m^{n_m} \bigotimes_{q=1}^{m} D_q |n_1, n_2, \dots, n_m\rangle \\ &= \sum_{n=0}^{\infty} \frac{c_n}{m^{n/2}} \sum_{n_1+\dots+n_m=n} \sqrt{\binom{n}{n_1, n_2, \dots, n_m}} |n_1, n_2, \dots, n_m\rangle,\end{aligned}$$

which is the expression for the output state of a balanced MBS, according to Eqs. (1) and (2).

2. Schmidt rank of $|\Phi_N\rangle$

We show that the Schmidt rank of $|\Phi_N\rangle$ is $N + 1$. According to Observation 3, we have the following SLOCC equivalences $|\Psi\rangle \sim |\Phi\rangle \sim |\Phi_N\rangle \sim |\Psi_N\rangle$; since the Schmidt rank is invariant under SLOCC, this implies that the Schmidt rank of the output state (1) is $N + 1$ as well.

Without loss of generality, let us consider an arbitrary bipartition $(\mathcal{H}_1 \otimes \mathcal{H}_2 \otimes \dots \otimes \mathcal{H}_{k-1}) \otimes (\mathcal{H}_k \otimes \mathcal{H}_{k+1} \otimes \dots \otimes \mathcal{H}_m)$ of the global state space $\mathcal{H}$. The Schmidt decomposition of the state $|\Phi_N\rangle$ corresponding to this bipartition is given by

$$\begin{aligned}|\Phi_N\rangle = |00\dots00\rangle &\otimes \left(\sum_{n_k+n_{k+1}+\dots+n_m=N} |n_k, n_{k+1}, \dots, n_m\rangle \right) \\ &+ \left(\sum_{n_1+n_2+\dots+n_{k-1}=1} |n_1, n_2, \dots, n_{k-1}\rangle \right) \otimes \left(\sum_{n_k+n_{k+1}+\dots+n_m=N-1} |n_k, n_{k+1}, \dots, n_m\rangle \right) \\ &+ \left(\sum_{n_1+n_2+\dots+n_{k-1}=2} |n_1, n_2, \dots, n_{k-1}\rangle \right) \otimes \left(\sum_{n_k+n_{k+1}+\dots+n_m=N-2} |n_k, n_{k+1}, \dots, n_m\rangle \right) \\ &+ \dots + \left(\sum_{n_1+n_2+\dots+n_{k-1}=N} |n_1, n_2, \dots, n_{k-1}\rangle \right) \otimes |00\dots00\rangle.\end{aligned}$$

Since for any bipartition of $\mathcal{H}$ the number of terms in the Schmidt decomposition above is $N + 1$, we conclude that the Schmidt rank of $|\Phi_N\rangle$ is $N + 1$.

[1] M. A. Nielsen and I. L. Chuang, *Quantum Computation and Quantum Information* (Cambridge University Press, Cambridge, England, 2000).
[2] R. Horodecki, P. Horodecki, M. Horodecki, and K. Horodecki, Rev. Mod. Phys. **81**, 865 (2009).
[3] C. Ritz, *Characterizing the Structure of Multiparticle Entanglement in High-Dimensional Systems*, Ph.D. thesis, University of Siegen (2019).
[4] O. Gühne and G. Tóth, Phys. Rep. **474**, 1 (2009).
[5] L. Amico, R. Fazio, A. Osterloh, and V. Vedral, Rev. Mod. Phys. **80**, 517 (2008).
[6] M. Sanz, I. L. Egusquiza, R. Di Candia, H. Saberi, L. Lamata, and E. Solano, Sci. Rep. **6**, 30188 (2016).
[7] A. Cabello, Phys. Rev. A **65**, 032108 (2002).
[8] W. Dür, G. Vidal, and J. I. Cirac, Phys. Rev. A **62**, 062314 (2000).

[9] A. Miyake, Phys. Rev. A **67**, 012108 (2003).
[10] F. Verstraete, J. Dehaene, and B. De Moor, Phys. Rev. A **68**, 012103 (2003).
[11] L. Lamata, J. Leon, D. Salgado, and E. Solano, Phys. Rev. A **74**, 052336 (2006).
[12] X. Li and D. Li, Phys. Rev. Lett. **108**, 180502 (2012).
[13] G. Gour and N. R. Wallach, Phys. Rev. Lett. **111**, 060502 (2013).
[14] F. E. S. Steinhoff, Phys. Rev. A **100**, 022317 (2019).
[15] S. Kumar, D. Bhatti, A. E. Jones, and S. Barz, New J. Phys. **25**, 063027 (2023).
[16] D. Bhatti and S. Barz, Phys. Rev. A **107**, 033714 (2023).
[17] N. Killoran, F. E. S. Steinhoff, and M. B. Plenio, Phys. Rev. Lett. **116**, 080402 (2016).
[18] B. Regula, M. Piani, M. Cianciaruso, T. R. Bromley, A. Streltsov, and G. Adesso, New J. Phys. **20**, 033012 (2018).
[19] J. K. Asbóth, J. Calsamiglia, and H. Ritsch, Phys. Rev. Lett. **94**, 173602 (2005).
[20] J. S. Ivan, S. Chaturvedi, E. Ercolessi, G. Marmo, G. Morandi, N. Mukunda, and R. Simon, Phys. Rev. A **83**, 032118 (2011).
[21] M. Owari, K. Matsumoto, and M. Murao, Phys. Rev. A **70**, 050301(R) (2004).
[22] Z. Li, Y.-G. Han, H.-F. Sun, J. Shang, and H. Zhu, Phys. Rev. A **103**, 022601 (2021).
[23] R. I. Nepomechie and D. Raveh, arXiv:2301.04989.
[24] J. Romero-Pallejà, J. Ahiable, A. Romancino, C. Marconi, and A. Sanpera, arXiv:2403.05244.
[25] R. I. Nepomechie, F. Ravanini, and D. Raveh, arXiv:2402.03233.
[26] N. Gisin, Phys. Lett. A **210**, 151 (1996).
[27] J. Bowles, J. Francfort, M. Fillettaz, F. Hirsch, and N. Brunner, Phys. Rev. Lett. **116**, 130401 (2016).
[28] G. Vidal, Phys. Rev. Lett. **83**, 1046 (1999).
[29] Y. Huang, H. Yu, F. Miao, T. Han, and X. Zhang, Int. J. Quantum Inf. **20**, 2150035 (2022).
[30] J. Chang, N. Jing, and T. Zhang, Int. J. Theor. Phys. **62**, 6 (2023).
[31] S. Wang, Y. Lu, M. Gao, J. Cui, and J. Li, J. Phys. A: Math. Theor. **46**, 105303 (2013).
[32] R. R. Puri, *Mathematical Methods of Quantum Optics* (Springer, Berlin, 2001).
[33] F. E. S. Steinhoff *et al.* (unpublished).
[34] A. Z. Goldberg and D. F. V. James, J. Phys. A: Math. Theor. **51**, 385303 (2018).
[35] M. C. Tichy, F. Mintert, and A. Buchleitner, Phys. Rev. A **87**, 022319 (2013).
[36] M. Koniorczyk, Z. Kurucz, A. Gábris, and J. Janszky, Phys. Rev. A **62**, 013802 (2000).
[37] W. Leoński and A. Kowalewska-Kudlaszyk, Prog. Opt. **56**, 131 (2011).
[38] J. J. Guanzon, M. S. Winnel, A. P. Lund, and T. C. Ralph, Phys. Rev. Lett. **128**, 160501 (2022).
[39] F. E. S. Steinhoff, M. C. de Oliveira, J. Sperling, and W. Vogel, Phys. Rev. A **89**, 032313 (2014).
[40] R. A. Horn and C. R. Johnson, *Matrix Analysis* (Cambridge University Press, Cambridge, England, 1985).
[41] B. M. Terhal and P. Horodecki, Phys. Rev. A **61**, 040301(R) (2000).
[42] A. Sanpera, D. Bruss, and M. Lewenstein, Phys. Rev. A **63**, 050301(R) (2001).
[43] C. Zhang, S. Denker, A. Asadian, and O. Gühne, Phys. Rev. Lett. **133**, 040203 (2024).
[44] A. Acín, D. Bruss, M. Lewenstein, and A. Sanpera, Phys. Rev. Lett. **87**, 040401 (2001).
[45] C. Ritz, C. Spee, and O. Gühne, J. Phys. A: Math. Theor. **52**, 335302 (2019).
[46] B. Vlastakis *et al.*, Science **342**, 607 (2013).
[47] L. Mandel and E. Wolf, *Optical Coherence and Quantum Optics* (Cambridge University Press, Cambridge, England, 1995).
[48] K. Hoffman and R. Kunze, *Linear Algebra* (Prentice-Hall, Upper Saddle River, NJ, 1962).
[49] Lin Chen and Yi-Xin Chen, Phys. Rev. A **73**, 052310 (2006).
[50] L. Chen, Y.-X. Chen, and Y.-X. Mei, Phys. Rev. A **74**, 052331 (2006).
[51] K. C. Tan and H. Jeong, Quantum Rep. **1**, 151 (2019).
[52] M. Engelkemeier, J. Sperling, J. Tiedau, S. Barkhofen, I. Dhand, M. B. Plenio, B. Brecht, C. Silberhorn, arXiv:2105.03720.
[53] B. Mendei, G. Homa, P. Ádám, and M. Koniorczyk, arXiv:2406.19207.
[54] S. Chin, J. Ryu, and Y.-S. Kim, arXiv:2406.10830.
[55] P. V. Parellada, V. G. Garcia, J.-J. Moyano-Fernández, and J. C. Garcia-Escartin, Results Phys. **54**, 107108 (2023).